

See discussions, stats, and author profiles for this publication at: <https://www.researchgate.net/publication/6950063>

Geometries, Thermodynamic Properties and Reactions of Methylzinc Alkoxide Clusters Studied by Density Functional Theory Calculations

ARTICLE *in* THE JOURNAL OF PHYSICAL CHEMISTRY A · JULY 2006

Impact Factor: 2.69 · DOI: 10.1021/jp060725a · Source: PubMed

CITATIONS

14

READS

24

2 AUTHORS:



Ralf Steudel

Technische Universität Berlin

357 PUBLICATIONS 4,602 CITATIONS

SEE PROFILE



Yana Steudel

John Wiley And Sons

38 PUBLICATIONS 301 CITATIONS

SEE PROFILE

Geometries, Thermodynamic Properties and Reactions of Methylzinc Alkoxide Clusters Studied by Density Functional Theory Calculations

Ralf Steudel* and Yana Steudel

Institut für Chemie, Technische Universität Berlin, Sekr. C2, D-10623 Berlin, Germany

Received: February 3, 2006; In Final Form: May 8, 2006

Methylzinc alkoxide complexes are precursors for the preparation of nanosized zinc oxide particles, which in turn are catalysts or reagents in important industrial processes such as methanol synthesis and rubber vulcanization. We report for the first time the structures, energies, atomic charges, dipole moments, and vibrational spectra of more than 20 species of the type $[(\text{MeZnOR}')_n]$ with $\text{R}' = \text{H}, \text{Me}, \text{'Bu}$ and $n = 1-6$, calculated by density functional theory methods, mostly at the B3LYP/6-31+G* level of theory. For $\text{R}' = \text{Me}$, the global minimum structure of the tetramer ($n = 4$) is a highly symmetrical heterocubane but a ladder-type isomer is by only 70.9 kJ mol^{-1} less stable. The corresponding trimer is most stable as a rooflike structure; a planar six-membered ring of relative energy 13.5 kJ mol^{-1} corresponds to a saddle point connecting two equivalent rooflike trimer structures. All dimers form planar four-membered Zn_2O_2 rings whereas the monomer has a planar CZnOC backbone. A hexameric drumlike structure represents the global minimum on the potential energy hypersurface of $[(\text{MeZnOMe})_6]$. The enthalpies and Gibbs energies of the related dissociation reactions hexamer \rightarrow tetramer \rightarrow trimer \rightarrow dimer \rightarrow monomer as well as of a number of isomerization reactions have been calculated. The complexes $[(\text{MeZnOMe})_n]$ ($n = 1-3$) form adducts with Lewis bases such as tetrahydrofuran (thf) and pyridine (py). The binding energy of py to the zinc atoms is about 65% larger than that of thf but is not large enough to break up the larger clusters. The bimolecular disproportionation of $[(\text{MeZnOMe})_4]$ with formation of the dicubane $[\text{Zn}\{(\text{MeZn})_3(\text{OMe})_4\}_2]$ and Me_2Zn is less endothermic than any isomerization or dissociation reaction of the heterocubane, but for steric reasons this reaction is not possible if $\text{R}' = \text{'Bu}$. A novel reaction mechanism for the reported interconversion, disproportionation and ligand exchange reactions of zinc alkoxide complexes is proposed.

1. Introduction

Zinc alkoxide clusters are useful precursors for the chemical vapor deposition of zinc materials, especially for the preparation of catalytically active ZnO nanoparticles.^{1,2} For this reason, there has been considerable recent interest in the synthesis and characterization of such species³⁻⁷ and of related compounds with (partly) inorganic substituents such as trimethylsilyl groups.^{8,9} However, a systematic investigation on the relative thermodynamic stability as a function of the cluster size and of the presence or absence of donor molecules such as tetrahydrofuran or pyridine is lacking. Furthermore, the primary reactions on heating as well as the potential intermediates of the thermolysis are only poorly understood.

A large number of substituted zinc oxide clusters of the general type $[(\text{RZnOR}')_n]$ with $\text{R}, \text{R}' = \text{alkyl or aryl}$ and $n = 2-6$ has been prepared but only in a few cases the molecular structures have been determined crystallographically. One of the first and probably the best known example is the tetrameric cluster $[(\text{MeZnOMe})_4]$ obtained by methanolysis of dimethylzinc.¹⁰ This molecule contains a cubanelike Zn_4O_4 core of approximately tetrahedral symmetry.¹¹ The most stable size of the Zn_nO_n clusters in the reported molecules depends on the steric requirements of the substituents as the preparation of the trimeric species $[(\text{MeZnO}^i\text{Bu})_3]$ and of the dimeric complexes $[(\text{EtZnOC}_6\text{F}_5)_2]$ and $[(\text{EtZnOC}_6\text{Cl}_5)_2]$ demonstrates.¹² In addition, the adduct formation with pyridine (py) or TMEDA

(tetramethylenediamine) evidently favors smaller cluster sizes as in $[(\text{EtZnOPh})_2 \cdot 2\text{py}]$, $[(\text{EtZnOC}_6\text{F}_5)_2 \cdot 2\text{py}]$, $[\text{EtZnOC}_6\text{F}_5 \cdot \text{TMEDA}]$ and $[\text{EtZnOC}_6\text{Cl}_5 \cdot 2\text{py}]$.¹² In all of these cases, the state of aggregation has been determined by molecular weight determination in solution and molecular or crystal structures have not been reported.

In this work, we have studied by theoretical methods the structures, relative energies, vibrational spectra, atomic charges and some important reactions of more than 20 methylzinc alkoxide clusters $[(\text{MeZnOR})_n]$ with n ranging from 1 to 6 and R being hydrogen, methyl (Me) or *tert*-butyl (*t*Bu). The results provide a new insight into the so-far ill-understood thermal reactions as well as the disproportionation and ligand exchange reactions of these clusters.

2. Experimental Section

2.1. Computational Details. Ab initio calculations were carried out with the GAUSSIAN 03 series of programs¹³ at the B3LYP level of theory using the basis sets 3-21G*, 6-31G*, 6-31+G*, 6-31G(2df,p), 6-31+G(2df,p) and 6-311++G(3df,3pd).¹⁴ In some cases, the BP86/6-311++G* method was applied. No symmetry or geometry restrictions were applied in the geometry optimizations of the most stable structures. Open-shell molecules were calculated using the unrestricted B3LYP method.

For most of the investigated molecules, a charge density analysis was performed using the natural bond orbital (NBO) approach based on the B3LYP/6-31+G* wave function.¹⁵ NBO

* Corresponding author. E-mail: steudel@sulfur-research.de.

TABLE 1: Comparison of the Experimental and Calculated Properties of Dimethylzinc Using Three Different Basis Sets and the B3LYP Method (d = Bond Length; D_1 = First Homolytic Dissociation Enthalpy, ΔH°_{298} ; Last Column = Single Point Calculations on the 6-31G* Geometry)

property	experimental data	6-31G*	6-31G-(2df,p)	6-31+G*	6-31+G**//6-31G*
$d(\text{Zn}-\text{C})/\text{pm}$	193.0(2), ^a 192.9(4) ^b	192.1	191.2	195.5	192.1
$D_1(\text{Me}-\text{ZnMe})/\text{kJ mol}^{-1}$ (298 K)	266 ± 6 , ^c 285 ± 17 , ^d 276–298 ^e	326.6	327.3	283.1	284.3

^a Reference 17. ^b Reference 21. ^c Reference 18a. ^d Reference 18b. ^e Reference 18c.

TABLE 2: Comparison of the X-ray Diffraction Structure of the Cubanelike Molecule $[(\text{MeZnOMe})_4]$ with the Geometry Calculated by Differing DFT Methods and Using Different Basis Sets (Bond Distances in pm; Bond Angled in deg)

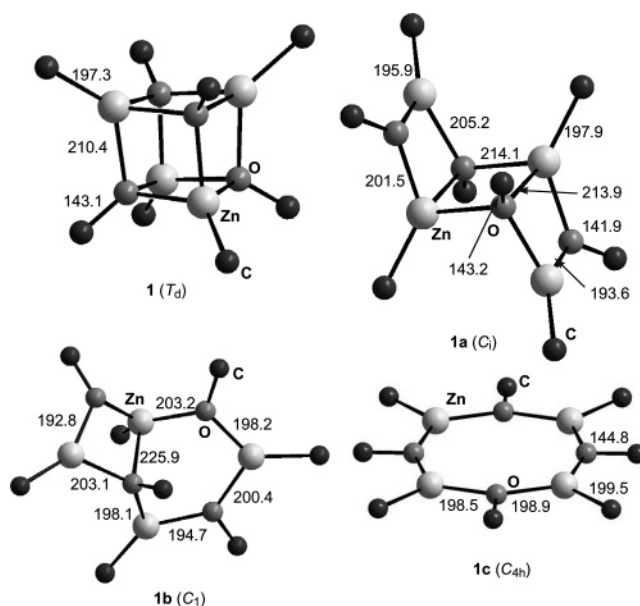
	Zn–O	Zn–C	C–O	O–Zn–O	Zn–O–Zn
solid state data ^a	207.8	194.6	143.4	83.8	95.9
B3LYP/6-31G*	206.6	194.8	142.7	82.6	96.0
B3LYP/6-31+G*	210.4	197.3	143.1	83.0	96.6
BP86/6-311++G*	210.7	196.8	143.9	82.7	96.9

^a Reference 11; averaged parameters.

atomic charges of small molecules have recently been demonstrated to agree well with experimental values obtained from X-ray diffraction data.¹⁶ All relative energies reported in this publication are given as ΔE at the potential energy minimum. Harmonic fundamental vibrations (unscaled) of all species were calculated at the same level as the corresponding geometry to characterize stationary points as equilibrium structures, with all frequencies real. The Gibbs reaction energies were obtained from the second law of thermodynamics, $\Delta G^\circ_T = \Delta H^\circ_T - T\Delta S^\circ_T$, where ΔS°_T is the entropy change and $\Delta H_T = \Delta H_0 + (H_T - H_0)$.

2.2. Reference Calculations. To find out which level of theory would reproduce the geometries and energies of the zinc alkoxide clusters best, we have carried out B3LYP calculations with the 6-31G*, 6-31+G* and 6-31G(2df,p) basis sets. Unfortunately, only very few reliable thermodynamic data for organozinc compounds are available as reference data. Therefore, the vapor phase geometry¹⁷ and the homolytic dissociation energy¹⁸ of dimethylzinc (Table 1) as well as the geometry² of the tetrameric cluster $[(\text{MeZnOMe})_4]$ (Table 2) were used. Within the framework of our computational resources the 6-31+G* basis set gave the best agreement between the experimental and calculated first dissociation enthalpy of Me_2Zn . The geometries of Me_2Zn and of $[(\text{MeZnOMe})_4]$ were reproduced equally well with the 6-31G* and 6-31+G* basis sets (see Tables 1 and 2). CBS-Q and G2(MP2) calculations on Me_2Zn gave less accurate data (CBS-Q: $d_{\text{Zn}-\text{C}} = 197.2$ pm, $D_1 = 337.7$ kJ mol⁻¹; G2(MP2): $d_{\text{Zn}-\text{C}} = 197.3$ pm, $D_1 = 308.7$ kJ mol⁻¹). Because we are mainly interested in reliable energies, the B3LYP/6-31+G* level was used in all reported geometry and energy calculations except for one of the largest clusters, namely, the dicubane **3**, which had to be calculated at the more economical B3LYP/6-31G* level for the geometry optimization followed by a single point energy calculation at the B3LYP/6-31+G* level. Thus, unless noted otherwise all reported energies and enthalpies refer to the B3LYP/6-31+G**//B3LYP/6-31+G* level of theory. The absolute energies, enthalpies and Gibbs energies of all species calculated in this work are given in Table S1 in the Supporting Information.

The calculated geometry of Me_2Zn is strictly linear (symmetry D_3)¹⁹ with the 2-fold degenerate C–Zn–C bending vibration

**Figure 1.** Structures and symmetries of the isomeric tetramers $[(\text{MeZnOMe})_4]$ (**1**, **1a**, **1b** and **1c**). The hydrogen atoms have been omitted for clarity. Bond lengths in pm.

at 138.5 cm⁻¹, in agreement with the experimental spectrum²⁰ and with previous determinations of the geometry by spectroscopic²¹ and theoretical²² methods. Reference calculations were also carried out using the BP86 method with the more flexible 6-311++G* basis set. However, both the geometry of Me_2Zn ($d_{\text{Zn}-\text{C}}$: 194.8 pm) and its first dissociation energy (300.6 kJ mol⁻¹ at 298 K) were less well reproduced than with the B3LYP/6-31+G* method. The same holds for the geometry of the cubane **1** (see Table 2). Therefore, we did not use this method in general.

3. Results and Discussion

In the following, we first report on the geometries of the various $[(\text{MeZnOR})_n]$ oligomers and their isomers. We then present our results on the structures of the tetrahydrofuran and pyridine adducts and on the interaction of MeZnOMe with benzene. The thermodynamic properties of the dissociation and association reactions, of the adduct formation as well as of some hydrolysis and condensation reactions are reported next. Finally, we discuss possible reaction mechanisms and the thermodynamics of the ligand exchange, interconversion and disproportionation reactions.

3.1. Geometries. **3.1.1. Tetrameric Clusters and Related Species.** The tetranuclear cluster molecule $[(\text{MeZnOMe})_4]$ (**1**) consists of a cubelike Zn_4O_4 core with the eight methyl groups jutting out in the direction of the 3-fold rotation axes of the core of T_d symmetry.¹¹ All non-hydrogen atoms are tetracoordinate; see Figure 1. We have confirmed this structure as the global energy minimum at all levels employed and, for the first time, determined the hydrogen positions. The Zn–O bonds are highly polar as the NBO atomic charges on the zinc atoms of +1.46 and on the oxygen atoms of –1.12 indicate. Nevertheless, the dipole moment of **1** is zero. For comparison, the atomic charge on zinc in Me_2Zn is +1.22 (carbon: –1.34). The fundamental vibrations of the $\text{Zn}_4\text{O}_4\text{C}_8$ skeleton of **1** are listed in Table 3.

Interestingly, the tetramer $[(\text{MeZnOMe})_4]$ exists as several isomeric structures on the potential energy hypersurface (PES). The tricyclic ladder-type structure of C_i symmetry (**1a** in Figure 1) can formally be generated from the cubane **1** by cleaving

TABLE 3: Vibrational Frequencies of $[(\text{CH}_3\text{ZnOCH}_3)_4]$ (1**) in the Region of the Skeleton Vibrations, Calculated at the B3LYP/6-31+G* Level**

degeneracy	wavenumber (cm^{-1})	assignment
2	145	COZn bending
3	150	OZnO bending
1	205	Zn_4 tetrahedron breathing
3	273	ZnOZn bending
3	295	ZnO stretching
1	325	O_4 tetrahedron breathing
2	346	COZn bending and ZnO stretching
3	402	COZn bending and ZnO stretching
3	536	ZnC stretching
1	542	ZnC stretching

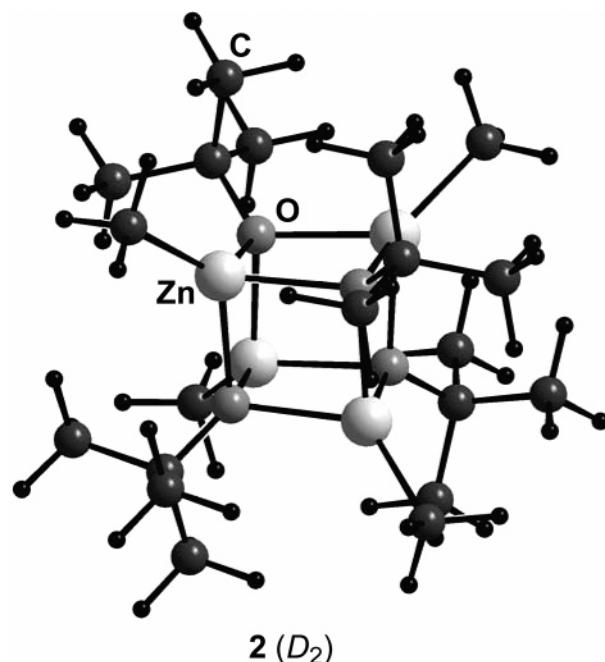
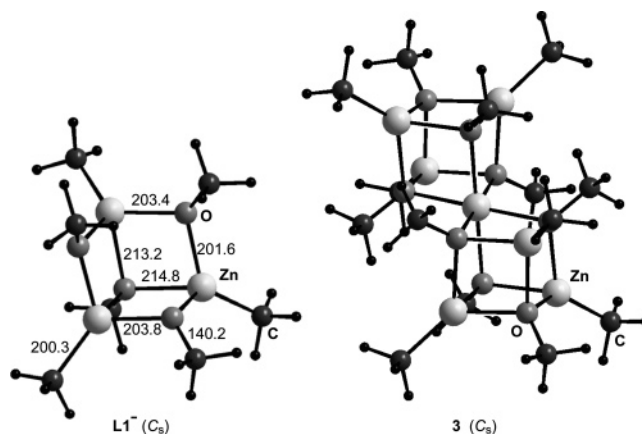
two parallel Zn–O bonds and opening the cube to form a ladder or band structure which corresponds to a local energy minimum. The relative energy ΔE of **1a** is just 70.9 kJ mol^{-1} ($\Delta H^\circ_{298} = 70.9 \text{ kJ mol}^{-1}$). The Gibbs energy (ΔG°_{298}) of 62.7 kJ mol^{-1} is equivalent to an equilibrium constant $K_c = c(\mathbf{1a})/c(\mathbf{1})$ of 4×10^{-12} at 25°C .

In isomer **1a**, two zinc atoms are four-coordinate and two are three-coordinate, the latter exhibiting a planar coordination sphere. The mean Zn–O distance of **1a** is 205.7 pm , i.e., 5 pm shorter than in isomer **1**. The central Zn_2O_2 unit is planar whereas the other two Zn_2O_2 rings exhibit torsion angles of $\pm 10.8^\circ$. In principle, isomer **1a** can be extended into longer or even infinite ladder structures by incorporating more and more tetramer units. The energy required for each incorporation step is expected to be much less than 71 kJ mol^{-1} because with increasing length of the ladder more and more zinc atoms will be four-coordinate as in the cubane tetramer. Evidently, the coordination number (CN) of 4 is energetically more favorable than CN = 3. The significance of such reactions will be outlined below.

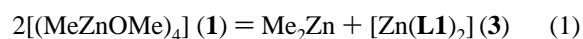
If three Zn–O bonds of **1** are cleaved the bicyclic tetramer **1b** is generated which is also a local minimum on the PES of $[(\text{MeZnOMe})_4]$ (see Figure 1) with a relative energy of $120.8 \text{ kJ mol}^{-1}$.

The global minimum structure of the unsubstituted Zn_4O_4 molecule is a planar eight-membered ring with alternating Zn and O atoms.²³ Therefore, we have investigated whether the corresponding methyl-substituted structure with all non-hydrogen atoms in one plane is a local minimum on the PES of $[(\text{MeZnOMe})_4]$. Such a structure can formally be generated from the cubane **1** by cleaving four Zn–O bonds. However, on geometry optimization without any symmetry restrictions this planar structure collapsed to the cubane **1**. When the planarity of the eight-membered ring was enforced by restricting all Zn–O–Zn–O torsion angles to 0° the geometry optimization resulted in a structure of C_{4h} symmetry (**1c**) with five imaginary frequencies (relative energy $233.9 \text{ kJ mol}^{-1}$); see Figure 1. The imaginary frequencies belong to out-of-plane torsion modes of the non-hydrogen atoms.

Several derivatives of **1** with bulkier organic groups at the oxygen atoms have been prepared.^{3,11,24,25} To check the influence of a sterically more demanding substituent, we have calculated the hitherto unknown structure of the complex $[(\text{MeZnO}^t\text{Bu})_4]$ (**2**), which is shown in Figure 2. The exact symmetry of **2** is C_2 but is very close to D_2 ($\mu = 0.00 \text{ D}$). The bonds Zn–O and Zn–C are by 0.9 and 1.0 pm , respectively, longer than in **1**; however, the C–O bond is 2.8 pm longer than in **1**. There are several close contacts of 252.0 pm between the hydrogen atoms of neighboring methyl and *tert*-butyl groups. Consequently, the Zn_4O_4 core of **2** is sterically well protected by the eight alkyl groups.

**Figure 2.** Structure of $[(\text{MeZnO}^t\text{Bu})_4]$ (**2**). Bond lengths (pm): Zn–O 211.4 , Zn–C 198.3 , C–O 145.9 . Bond angles (deg): Zn–O–Zn 95.4 , O–Zn–O 84.3 , O–Zn–C 129.3 , Zn–O–C 121.3 .**Figure 3.** Structures of the ligand $[(\text{MeZn})_3(\text{OMe})_4]^-$ (**L1**) and of the related dicubane $[\text{Zn}\{(\text{MeZn})_3(\text{OMe})_4\}_2]$ (**3**). Bond lengths in pm.

In some of the first extensive investigations of the methanolysis of dimethylzinc,^{26,27} it was observed that in benzene solution the tetramer **1** is in equilibrium with dimethylzinc and the dicubane species $[\text{Zn}\{(\text{MeZn})_3(\text{OMe})_4\}_2]$ (**3**) shown in Figure 3. The latter complex is formally composed of a central hexacoordinate zinc dication and two anionic ligands $[(\text{MeZn})_3(\text{OMe})_4]^-$. In the following, this tripod ligand will be denoted as **L1**:



The structure and atomic charges of **3** were investigated at the B3LYP/6-31G* level resulting in a structure of C_s symmetry with a mean Zn–O bond length of 206.3 pm at the four-coordinate zinc atoms and of 212.6 pm at the nearly octahedrally coordinated central atom. The corresponding values from the X-ray diffraction analysis on single crystals of **3** are 203.8 – 214.7 pm within the ligands and 206.8 – 217.0 pm at the central atom.²⁸ The mean O–Zn–O bond angles are calculated as 99.7° at the central atom between the two ligands (besides the 180° angles which are obvious), 83.3° at the four-coordinate zinc atoms and 80.3° at the central atom within each ligand **L1**. The

four atoms located on each of the 12 faces of the two cubes are not exactly in one plane as has been claimed for the molecular structure in the crystal but the corresponding torsion angles Zn–O–Zn–O amount to $\pm 6.5^\circ$ at the four-coordinate zinc atoms and $\pm 8.0^\circ$ if the six-coordinate metal atom is included. The crystallographic site symmetry is centrosymmetrical but not octahedral.²⁸ Due to the lack of intermolecular forces, our calculated structure is much more regular because the range of Zn–O bond distances is much smaller than reported for the solid-state structure. If some of the hydrogen atoms are ignored, our structure of **3** is also centrosymmetrical.

The shortest interligand distance between the methyl groups of the two η^3 -ligands of **3** is 240.8 pm, which is about the van der Waals distance between two hydrogen atoms. From these data and from the investigation of appropriate model molecules it is evident that derivatives of **3** with *all* alkoxy groups sterically more demanding as in the case of $-\text{O}^i\text{Pr}$ and in particular with $-\text{O}^i\text{Bu}$ will not be stable due to steric crowding. In fact, no dicubane clusters of these types have been prepared yet. However, there might be no problems if only *one* or *two* bulky groups are present in addition to several methoxy groups. The interligand O–Zn–O bond angles of 99.7° at the central atom of **3** also indicate that there is a certain repulsion between the two ligands **L1**. The NBO atomic charges of the six- and four-coordinate zinc atoms of **3** are +1.66 and +1.48, respectively, whereas the oxygen atoms bear a charge of -1.12 electrostatic units ($\mu = 0.12$ D).

The structure of the free chelate ligand $[(\text{MeZn})_3(\text{OMe})_4]^-$ (Figure 3) was investigated with the 6-31+G* basis set. The geometry is quite different from that of the related cluster **1** and similar to the structure of the trimer **4**, but with one additional methoxide anion. The only element of symmetry is a mirror plane (point group C_s ; $\mu = 1.23$ D). Two of the methyl groups at the three-coordinate oxygen atoms are bent “inwards”, i.e., toward the empty position where the zinc atom of the Zn_4O_4 cubane is “missing”. The Zn–O bond lengths of **L1** range from 203.4 to 214.8 pm and the nonbonding O...O distances between the three-coordinate oxygen atoms are 312.2 pm (twice) and 319.6 pm. The atomic charges on the three-coordinate oxygen atoms (-1.07), on the four-coordinate oxygen (-1.10) and on the zinc atoms ($+1.51$) are not much different from those of the cubane **1** (O: -1.12 ; Zn: $+1.46$), despite the anionic charge.

3.1.2. Trimeric and Hexameric Clusters. To the best of our knowledge, there are no reports on the structure of the trimeric cluster $[(\text{MeZnOMe})_3]$ (**4**) or of any derivative thereof with other organic substituents (alkyl or aryl) lacking donor atoms such as nitrogen or oxygen. However, the preparation of related trimeric cluster molecules of the type $[(\text{RZnOR})_3]$, e.g., with $\text{R} = {}^i\text{Bu}$,¹² and the preparation and X-ray crystallographic structure of the hydroxo complex $[(\text{RZnOH})_3]$ containing a Zn_3O_3 ring have been reported [with $\text{R} = \eta^2\text{-H}_2\text{B}(3\text{-C}_3\text{N}_2\text{H}_2{}^i\text{Bu})$].²⁹ The latter molecule is approximately of C_3 symmetry and the metallacycle is either planar or almost so.

The most stable structure of **4** is not a six-membered ring, as could have been expected from the geometry of unsubstituted Zn_3O_3 . Instead, species **4** has a rooflike geometry with four of the skeleton atoms three-coordinate and the other two four-coordinate (Figure 4). The molecular symmetry is C_s , resulting in a dipole moment of 0.77 D. Formally, this structure can be derived from the cubane **1** by removing one monomeric unit MeZnOMe , i.e., one edge of the cube. The two four-membered rings of **4** are almost planar (the torsion angles Zn–O–Zn–O are smaller than $\pm 8^\circ$). The angle between the two four-membered rings is about 105° . In **4**, the Zn–O bonds are no

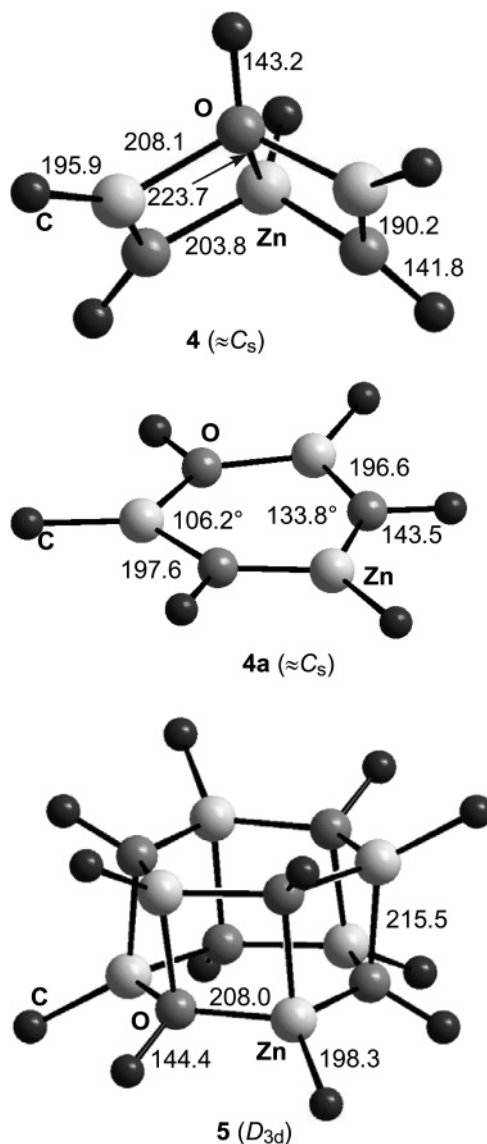


Figure 4. Structures of the trimeric species $[(\text{MeZnOMe})_3]$ (**4**) and of the hexamer $[(\text{MeZnOMe})_6]$ (**5**). The hydrogen atoms have been omitted for clarity. Bond lengths in pm.

longer identical as in **1** but can be classified in four groups (averaged for C_s symmetry): two short bonds (190.3 pm), two of intermediate length (203.65 pm), two slightly longer ones (208.2 pm), and one considerably longer one (223.7 pm). The average Zn–O bond length of 204.0 pm is smaller than in the tetramer **1** (210.4 pm; Table 2). The coordination sphere at the three-coordinate ring atoms is exactly planar. The positive charge on the three-coordinate zinc atoms (1.44) is slightly smaller than on the tetracoordinate atoms (1.48).

During the search for other structures on the PES of $[(\text{MeZnOMe})_3]$, we have located an isomer (**4a**) which has all non-hydrogen atoms and six of the hydrogens in one plane (symmetry C_{3h}); see Figure 4. However, this structure represents a saddle point with two imaginary frequencies connecting two equivalent rooflike geometries **4**. The energy of **4a** is just 13.5 kJ mol^{-1} higher than that of **4** (at the potential energy minimum). A first-order transition state of practically the same relative energy was also located. The remarkably low relative energy seems to be in contrast to the three-coordination of all ring atoms of **4a**. On the other hand, the Zn–O bonds of **4a** are considerably shorter (196.6 pm) than those of **4** (mean bond length: 204.0 pm), indicating a higher bond energy that

evidently helps to stabilize this structure. It should be noted that in the case of the unsubstituted Zn_3O_3 molecule the corresponding planar six-membered ring is the global minimum structure,²³ and the cited structure of $[(\text{RZnOH})_3]$ containing a planar Zn_3O_3 ring [$\text{R} = \eta^2\text{-H}_2\text{B}(3\text{-C}_3\text{N}_2\text{H}_2\text{Bu})$]²⁹ also indicates that the energy difference between ring and roof-shaped isomers must be small.

The small relative energy of **4a** has interesting consequences. For example, an interconversion of **4** via **4a** to an equivalent rooflike structure of **4** can be expected to take place at ambient temperatures in solution. Because all zinc atoms of **4a** are equivalent, this “inversion” of **4** makes all zinc atoms of **4** also equivalent on a not-too-short time scale. The same holds for the oxygen and carbon atoms.

If two molecules of **4a** are placed on top of each other with zinc on top of oxygen and vice versa, a drumlike hexamer is created. A structure of this type is in fact a local minimum on the PES of unsubstituted Zn_6O_6 .²³ The related hexameric cluster $[(\text{PhZnONEt}_2)_6]$ has been prepared, but no structure has been reported,¹² and the cation $[(\text{MeZnOEt})_6]^+$ has been observed in the EI mass spectrum of $[(\text{MeZnOEt})_4]$ at high temperatures.³⁰ We have found a minimum energy structure of $[(\text{MeZnOMe})_6]$ (**5**) which has the shape of a pseudohexagonal Zn_6O_6 drum with the methyl groups sticking out (see Figure 4). The symmetry of **5** is approximately D_{3d} (centrosymmetric). The two six-membered Zn_3O_3 rings are almost planar (torsion angles $\pm 4^\circ$) but the carbon atoms are not coplanar with the Zn_3O_3 rings. In other words, the geometry at the ring atoms is distorted tetrahedral with $\text{Zn}-\text{C}$ distances of 198.3 pm and $\text{C}-\text{O}$ distances of 144.4 pm. The $\text{Zn}-\text{O}$ distances within the Zn_3O_3 rings are shorter (208.0 pm) than those between the two rings (215.5 pm). The NBO atomic charge on the zinc atoms of **5** (+1.48) is larger than for any other neutral complex $[(\text{MeZnOMe})_n]$ investigated in this work.

3.1.3. Dimeric Clusters and Related Species. Numerous dimeric complexes of the type $[(\text{RZnOR}')_2]$ have been reported. The two complexes $[(\text{EtZnOC}_6\text{F}_5)_2]$ and $[(\text{EtZnOC}_6\text{Cl}_5)_2]$ have been the first examples, but no structure determinations have been published.¹² However, molecular and crystal structures are available for $[(\text{RZnO}\{2,6\text{-C}_6\text{H}_3\text{Pr}_2\})_2]$ and $[(\text{RZnO}\{2,4,6\text{-C}_6\text{H}_2\text{-Bu}_3\})_2]$ with $\text{R} = \text{CH}_2\text{SiMe}_3$. These compounds contain planar Zn_2O_2 heterocycles with $\text{Zn}-\text{O}$ bond lengths varying between 193.4 and 202.1 pm.³

Evidently, sterically rather demanding ligands on both the oxygen and zinc atoms enforce the smaller cluster size compared to the fully methyl-substituted species studied in this work, which prefers the heterocubane structure. On the other hand, the complex $[(\text{RZnOR}')_4]$ with $\text{R} = \text{CH}_2\text{SiMe}_3$ and $\text{R}' = \text{adamantyl}$ has been reported to be tetrameric.³

The most stable structure of the unsubstituted Zn_2O_2 molecule is a planar four-membered ring.²³ The two dimers studied in this work, $[(\text{MeZnOMe})_2]$ (**6**) and $[(\text{MeZnO}^i\text{Bu})_2]$ (**7**), adopt a similar structure with all non-hydrogen atoms in one plane; see Figure 5.

Species **6** is of C_i symmetry with $\text{Zn}-\text{O}$ bonds of length 197.2 pm (197.5 pm in **7**) and NBO atomic charges of +1.45 on zinc and -1.12 on the oxygen atoms. The same high polarity is found for the $\text{Zn}-\text{C}$ bonds because the methyl carbon atoms bear a charge of -1.34 electrostatic units, in contrast to the alkoxy carbon atoms with just -0.31 units. The bond angles within the heterocycle of **7** are 80.3° at zinc and 99.7° at oxygen. These data are in excellent agreement with the cited structures of the two dimeric complexes reported by Power et al.³ The most

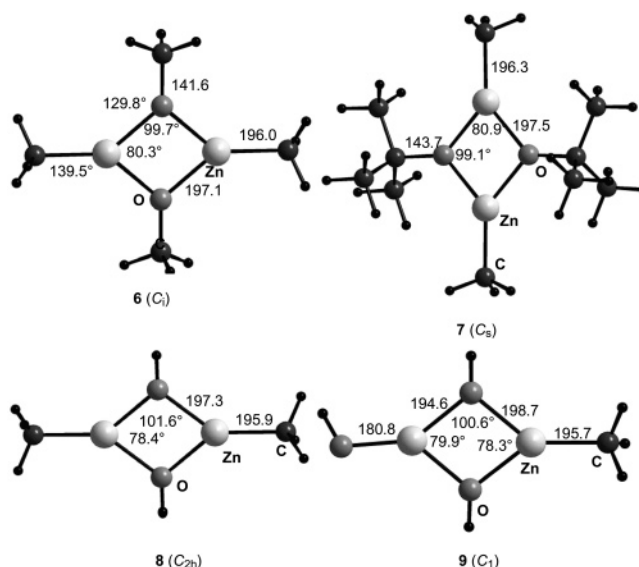


Figure 5. Structures of the dimeric complexes $[(\text{MeZnOMe})_2]$ (**6**), $[(\text{MeZnO}^i\text{Bu})_2]$ (**7**), $[(\text{MeZnOH})_2]$ (**8**) and $[\text{Zn}_2\text{Me}(\text{OH})_3]$ (**9**). Bond lengths in pm.

interesting vibrational frequencies of **6** are given in Table S2. The *tert*-butyl-substituted derivative **7** is of C_s symmetry.

We found that a chainlike isomer (**6a**) is also a stable species on the PES of $[\text{Zn}_2\text{O}_2\text{Me}_4]$. This molecule consists of two monomers connected by one coordinate $\text{Zn}-\text{O}$ bond of length 214.9 pm and one weak $\text{CH}\cdots\text{O}$ hydrogen bridge (see Figure 6). All non-hydrogen atoms are located in one plane (symmetry C_s , $\mu = 3.98$ D). Although one $\text{Me}-\text{Zn}-\text{O}$ bond angle is almost linear (179.5°), the other monomeric unit is bent at the zinc atom (160.7°). The relative energy of **6a** is 93.1 kJ mol^{-1} , which may approximately be identified with the ring opening energy of the cyclic dimer **6**.

Chemically and structurally related to the cyclic dimers **6** and **7** are the dinuclear hydroxy complex $[(\text{MeZnOH})_2]$ (**8**) and its hydrolysis product **9**:



The dihydroxy complex **8** may be generated from **7** by thermolysis with elimination of isobutene:



The structures of the model compounds **8** and **9** are shown in Figure 5. Except for the methyl-hydrogen atoms, both molecules are planar. The exocyclic $\text{Zn}-\text{O}(\text{H})$ bond of **9** (180.8 pm) is much shorter than the bonds within the ring (198.7 and 194.6 pm); the dipole moment is 2.19 D. The chemical significance of these compounds will be outlined below.

3.1.4. Monomeric Species $[\text{RMeZnR}']$. We have studied two monomeric species, $[\text{MeZnOMe}]$ (**10**) and $[\text{MeZnO}^i\text{Bu}]$ (**11**). Their hitherto unknown structures are shown in Figure 6 (symmetry C_s in both cases). Surprisingly, the bond angle at the zinc atoms of both monomers is not 180° as in dialkylzinc molecules¹⁷ and in the monomeric $\text{Zn}(\text{OH})_2$ molecule³¹ but slightly smaller, 174.3° in **10** and 174.6° in **11**. On the other hand, the bond angle at the oxygen atoms (130.1° in **10**, 130.5° in **11**) is considerably larger than in the H_2O molecule (104.5°) and in dimethyl ether (111.7°). The larger bond angle and the shorter $\text{Zn}-\text{O}$ bond may be taken as an indication of a coordinate π bond between the oxygen $2p_\pi$ lone pair and the unoccupied low-lying $4p_\pi$ orbital of the zinc atom. However,

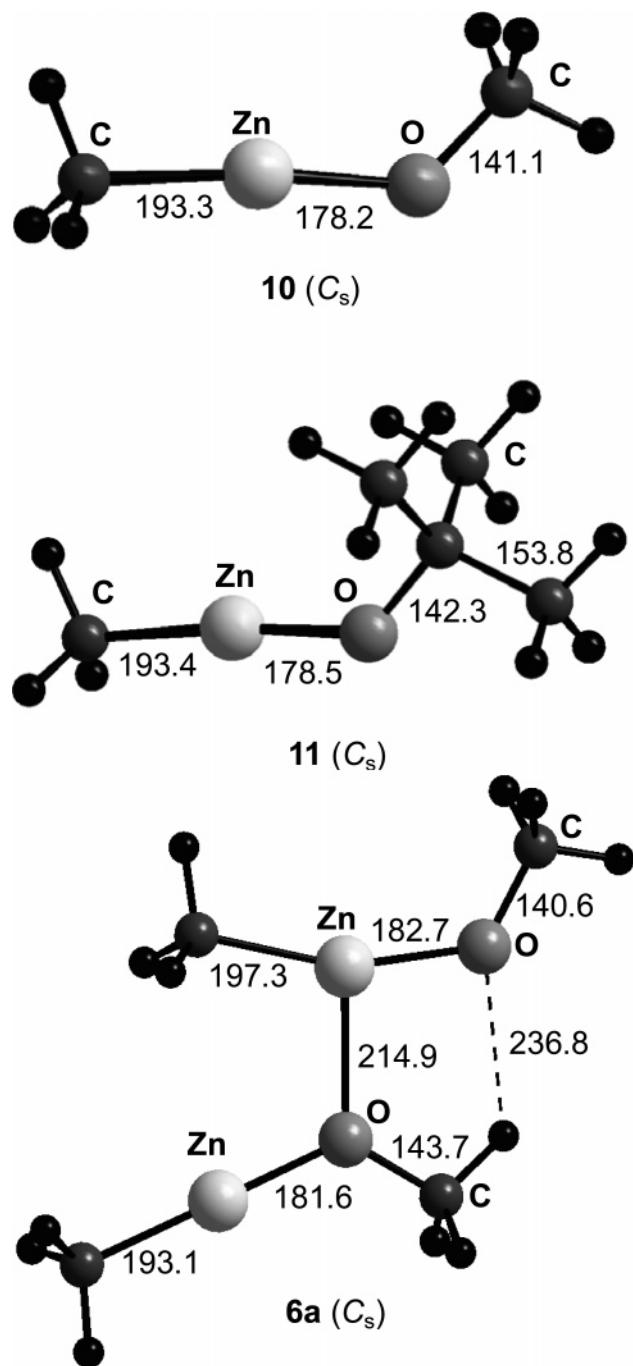


Figure 6. Structures of the chainlike dimer $[(\text{MeZnOMe})_2]$ (**6a**) and of the monomeric species $[\text{MeZnOMe}]$ (**10**) and $[\text{MeZnO}^i\text{Bu}]$ (**11**). Bond lengths in pm.

the HOMO of **10** shows only a weak sign of such a π bond. The torsion angles $\text{C}-\text{O}-\text{Zn}-\text{C}$ are 180° in both molecules **10** and **11**. The planar zigzag backbone of monomer **10** persisted also at higher levels of theory, e.g., with the much larger basis set 6-311++G(3df,3pd) resulting in the bond angles $\text{C}-\text{Zn}-\text{O} = 174.4^\circ$ and $\text{Zn}-\text{O}-\text{C} = 130.2^\circ$. The 3-fold rotation axis of the methyl group attached to the zinc atom is probably responsible for the deviation from linearity because the environment of the zinc atom within the molecular plane is different on both sides of this atom (see Figure 5). Most likely, the potential energy surface for the bending motion at the zinc atom is very flat. The corresponding in-plane $\text{C}-\text{Zn}-\text{O}$ bending frequency has been calculated as 98 cm^{-1} (see Table 4).

Though the methyl group attached to the zinc atom of **10** does not show any tilt,³² the methoxy group is tilted with

TABLE 4: Vibrational Frequencies of $[\text{CH}_3\text{ZnOCH}_3]$ (10**) in the Region below 1200 cm^{-1} , Calculated at the B3LYP/6-311++G(3df,3pd) Level**

symmetry species	wavenumber (cm^{-1})	assignment
a''	21	CO and CZn torsion
a''	69	CO torsion
a'	98	CZnO and ZnOC bending
a''	140	CZnO and ZnOC bending
a'	214	ZnOC and CZnO bending
a'	502	ZnC and ZnO in-phase stretching
a'	636	ZnC and ZnO out-of-phase stretching
a''	721	CH_3 rocking
a'	723	CH_3 rocking
a'	1115	CO and ZnC out-of-phase stretching
a''	1174	HCO bending
a'	1195	HCO bending

$\text{H}-\text{C}-\text{O}$ bond angles of 108.6° and 112.5° (twice). This effect is usually explained by an interaction of the oxygen $2p_\pi$ lone pair with the neighboring (parallel) $2p$ orbital of the carbon atom which is responsible for the bonding to the two out-of-plane hydrogen atoms ($n \rightarrow \sigma^*$ hyperconjugation).³³ However, a simpler rationalization involves the repulsion between the oxygen $2p_\pi$ lone pair and the bonding electrons of the two $\text{C}-\text{H}$ bonds which are approximately in the same plane as the lone pair. The two methyl groups of the molecule are staggered to each other.

The $\text{Zn}-\text{O}$ bonds of **10** (178.2 pm) and **11** (178.5 pm) are considerably shorter than those of the homologous dimeric (197.1 pm), trimeric (204.0 pm) and tetrameric (210.4 pm) clusters (global minimum structures). In fact, the lower the degree of association, the shorter these bonds become as the result of the intramolecular $\text{Zn}-\text{O}$ π bond, which can operate only at low coordination numbers at the zinc atom(s). To a certain degree, this bond shortening on dissociation also holds for the $\text{Zn}-\text{C}$ bond whereas the $\text{C}-\text{O}$ bonds are much less affected. The charge difference between the zinc (+1.36) and the oxygen atoms (−1.04) of monomer **10** is smaller than for the dimers **6** (+1.45/−1.12) and **7** (+1.47/−1.14) as well as for the cubane **1** (+1.46/−1.12). This may be taken as another indication for the proposed $\text{O}(2p) \rightarrow \text{Zn}(4p)$ π -bond.

3.1.5. Adducts with Tetrahydrofuran. Alkylzinc alkoxy complexes with a coordination number of the zinc atoms smaller than 4 are expected to form additional coordinate bonds to suitable donors such as oxygen atoms of ethers or nitrogen atoms of amines. We have studied the coordination of tetrahydrofuran (thf) to the trimeric, dimeric and monomeric $[(\text{MeZnOMe})_n]$ species. The structures of representative examples of the thf adducts are shown in Figure 7.

The $[(\text{MeZnOMe})_n]$ complexes with $n = 1-3$ form adducts with either one or two thf molecules. In the case of the trimer the first solvent molecule adds from the top of the “roof” to one of the three-coordinate zinc atoms forming a $\text{Zn}-\text{O}$ bond of length 226.5 pm (structure **12** in Figure 6). The impact of this adduct formation on the geometry of the trimer is minimal except that the $\text{Zn}-\text{O}$ bonds neighboring to the bond to thf increase in length by 3.5 and 5.7 pm, respectively. A second thf molecule can coordinate accordingly.

On coordination of the first thf molecule to the dimer **6** the Zn_2O_2 ring is slightly distorted and no longer planar (torsion angles $\pm 7.3^\circ$). The bond to the ligand is almost perpendicular to a mean plane through the Zn_2O_2 ring. Except for the C_4H_8 unit of the thf molecule, complex **13** is of C_s symmetry. In contrast, the adduct $[(\text{MeZnOMe})_2 \cdot 2\text{thf}]$ (**14**) with two thf molecules is of C_i symmetry with a strictly planar Zn_2O_2

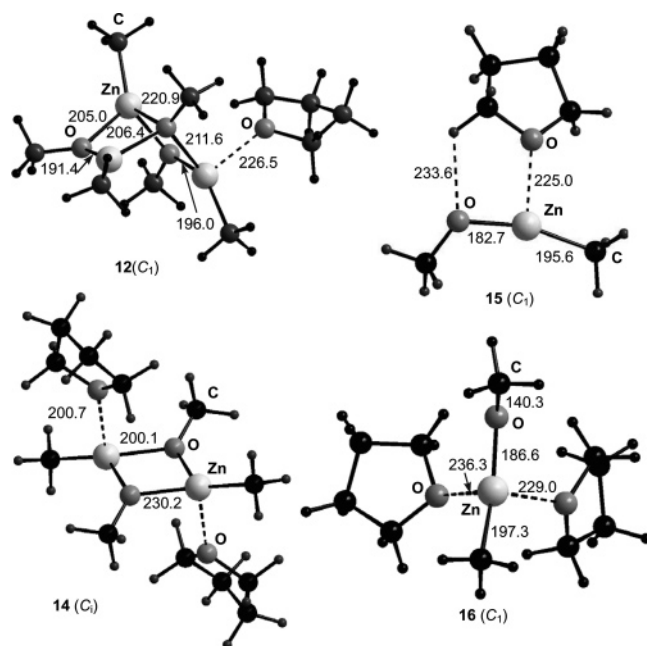


Figure 7. Structures of the tetrahydrofuran adducts [(MeZnOMe)₂·thf] (**12**), [(MeZnOMe)₂·2thf] (**14**), [MeZnOMe·thf] (**15**), and [MeZnOMe·2thf] (**16**). Bond lengths in pm.

heterocycle (Figure 7). However, the coordination sphere at the three-coordinate oxygen atoms of the ring is no longer planar (as in **6**) but slightly pyramidal. The coordination geometry at the zinc atoms is approximately tetrahedral with the Zn–O(thf) bond oriented almost perpendicular (94.5°) to the Zn₂O₂ plane. As expected, the average Zn–O bond length of 200.4 pm within the ring is much shorter than the Zn···O bonds to the thf ligands (230.2 pm). This thf···dimer interaction is predominantly a dipole-ion attraction between the positively charged zinc atoms of **6** (+1.45 electrostatic units) and the thf dipole moment, which was calculated as $\mu = 2.02$ D. This view is supported by the close agreement between the direction of the thf dipole vector and the Zn–O(thf) bond. As a consequence, the Zn–O bond length within the four-membered ring increases from 197.1 pm in **6** to 200.4 pm in **14** and the atomic charge on the zinc atoms increases to +1.49.

In the monomeric adduct [(MeZnOMe)·thf] the torsion angle C–Zn–O–C is no longer 180° as in the free molecule **10** but 5.5°. The geometry at the three-coordinate zinc atom is planar (sum of angles at Zn: 359.9°). In addition to the coordinative Zn···O interaction (225.0 pm) with the thf molecule, there is a weak H···O hydrogen bond of length 233.6 pm between one of the thf hydrogen atoms (at α -C) and the oxygen atom of the methoxy group. The corresponding adduct with two thf molecules (**16**) is also asymmetrical with two coordinate Zn···O bonds of lengths 229.0 and 236.3 pm and a (thf)O···Zn···O(thf) bond angle of 91.1°. The geometry of the monomeric MeZnOMe unit changes considerably on adduct formation with a bond angle C–Zn–O of 154.1° and a torsion angle of 15.2° (Figure 6). A similar interaction between thf molecules and a zinc atom has been observed in the related complex [Zn(OR)₂·2thf] (with R = 2,4,6-*i*-Bu₃H₂C₆) but both the Zn···O distances to the thf ligands (206.6 and 208.8 pm) and the Zn–O bonds to the OR ligands (188.5 and 188.9 pm) are much shorter.²⁵ The higher atomic charge on the metal atom of the latter complex can explain the difference in the bond lengths calculated for **16**.

3.1.6. Adducts with Pyridine. The formation of adducts of alkylzinc complexes of the type [(RZnOR')_n] with pyridine and

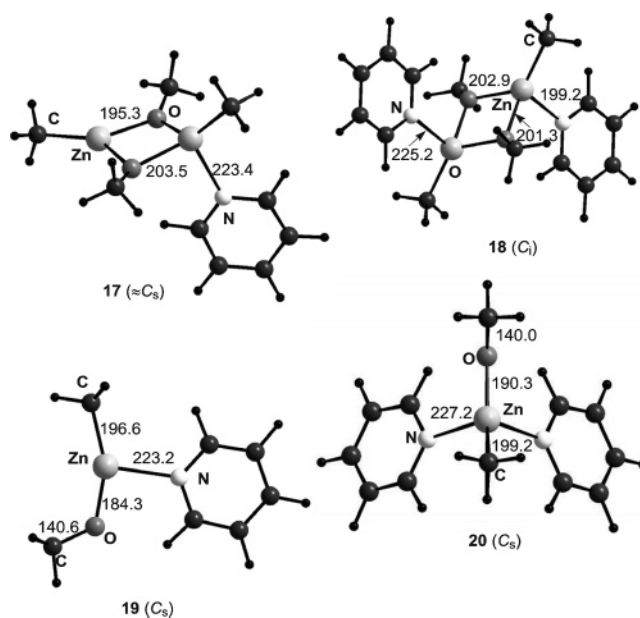


Figure 8. Structures of the complexes [(MeZnOMe)₂·py] (**17**), [(MeZnOMe)₂·2py] (**18**), [MeZnOMe·py] (**19**), and [MeZnOMe·2py] (**20**). Bond lengths in pm.

TMEDA (tetraethylenediamine) is well-known.¹² In these adducts, the zinc complex may be monomeric as in [EtZnOC₆F₅·TMEDA] and [EtZnOC₆Cl₅·2py], dimeric as in [(EtZnOPh)₂·2py] and [(EtZnOC₆F₅)₂·2py],¹² or trimeric as in [(RZnOC₂H₄NMe₂)₃], which contains an intramolecular nitrogen base.³⁴ To elucidate the structural principles of such compounds, we have studied the properties of the adducts [(MeZnOMe)₂·py] (**17**), [(MeZnOMe)₂·2py] (**18**), [MeZnOMe·py] (**19**), and [MeZnOMe·2py] (**20**); see Figure 8.

Species **17** is approximately of *C_s* symmetry ($\mu = 5.55$ D) with a Zn–N bond length of 223.4 pm and a Zn–Zn–N angle of 105.4°. The one-sided coordination of the pyridine molecule disturbs the Zn₂O₂ ring geometry considerably. The former planarity of the heterocycle is lifted with torsion angles Zn–O–Zn–O of $\pm 10.6^\circ$. On the other hand, the dinuclear complex [(MeZnOMe)₂·2py] (**18**) is of *C_i* symmetry. Though its Zn₂O₂ ring is strictly planar, the carbon atoms of the methoxy groups are located slightly above and below this plane.

In the mononuclear complex [MeZnOMe·py] (**19**) ($\mu = 4.90$ D) the C–Zn–O–C backbone is planar (torsion angle 0°), bent away from the pyridine ligand, and no longer zigzag shaped as in the free monomer **10**. The same holds for the derivative [MeZnOMe·2py] (**20**) which is also of *C_s* symmetry with $\mu = 6.36$ D. All bonds originating from the zinc atom are slightly shorter in **19** compared to **20** (Figure 7). Although the geometry at Zn is planar in **19**, a distorted tetrahedral coordination is predicted for **20** with the bond angles N–Zn–N = 94.1° and O–Zn–C = 146.0°.

An interesting related compound is the complex [(Me₃SiCH₂–ZnOCH₂{2-py})_n] containing a pyridine ligand linked to an oxygen atom of the Zn_nO_n core via a methylene group while being additionally coordinated to the zinc atom by its nitrogen atom. This remarkable substance is trimeric in benzene solution but tetrameric in the crystalline state as demonstrated by an X-ray crystallographic analysis. The tetramer contains a puckered eight-membered Zn₄O₄ ring with four-coordinate metal atoms.⁴

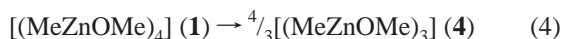
3.1.7. Adduct with Benzene. Benzene as a ligand is of interest because many preparative reactions of methylzinc alkoxides have been carried out in benzene²⁷ or toluene, and benzene may

serve as a model for toluene in quantum chemical calculations. The coordination of benzene to a positively charged zinc atom may take place via one of the CC bonds in a formally “side-on” geometry. However, the alkyl groups of the zinc complex hinder this type of approach of the planar benzene molecule. This holds in particular for the dimeric and trimeric zinc clusters studied in this work. For the monomeric MeZnOMe the steric problems are however minimal. In fact, a 1:1 “adduct” of **10** and C₆H₆ could be optimized as a minimum on the PES but the interaction energy was only 2.5 kJ mol⁻¹.

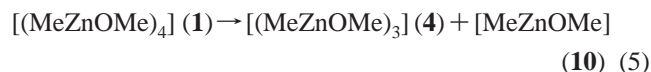
3.2. Thermodynamics. The structures, absolute energies and vibrational frequencies of all complexes were used to calculate the standard enthalpies and Gibbs energies of a number of important chemical reactions, starting with the dissociation of the larger clusters to give smaller species, followed by adduct formation with tetrahydrofuran (thf) and pyridine (py). This enabled us to determine the influence of adduct formation on the dissociation reactions of the cubane **1**. In addition, we were interested in hydrolysis and condensation reactions that are important steps in the transformation of **1** into zinc oxide nanoparticles. Finally, the previously observed ligand exchange and disproportionation reactions of cubane complexes had to be explained mechanistically.

3.2.1. Dissociation and Association Reactions. In this section, we report for the first time on the thermodynamics of the dissociation and association reactions of unsolvated [(MeZnOMe)_n] molecules with *n* = 1–4 and 6. Because the cubane **1** is the most stable species, all reactions are referred to this species (where appropriate). In solvents, on melting and in the vapor phase tetramers **1** and **2** could in principle dissociate into trimers, dimers or monomers. In addition, hexamers and other larger clusters may be produced because even polymeric [(MeZnOMe)_n] is known. In fact, all the mentioned nonpolymeric molecular sizes have been reported for compounds of the type [(RZnOR')_n] depending on the bulkiness of the substituents,¹² on the donor properties of the solvent³⁵ or of the organic ligands.^{12,36}

3.2.1.a. Dissociation of the Tetramers 1 and 2. All dissociation reactions of the heterocubanes **1** and **2** are strongly endothermic, but less so if bulky substituents such as ^tBu are part of the alkoxy groups. Of all dissociation pathways with formation of separated species the dimer formation is most favorable energetically, as the following data show.



$$\Delta H^\circ_{298} = 102.3 \text{ kJ mol}^{-1} \quad \Delta G^\circ_{298} = 58.3 \text{ kJ mol}^{-1}$$



$$\Delta H^\circ_{298} = 178.5 \text{ kJ mol}^{-1} \quad \Delta G^\circ_{298} = 102.2 \text{ kJ mol}^{-1}$$



$$\Delta H^\circ_{298} = 122.2 \text{ kJ mol}^{-1} \quad \Delta G^\circ_{298} = 34.2 \text{ kJ mol}^{-1}$$



$$\Delta H^\circ_{298} = 90.6 \text{ kJ mol}^{-1}$$



$$\Delta H^\circ_{298} = 406.8 \text{ kJ mol}^{-1} \quad \Delta G^\circ_{298} = 234.1 \text{ kJ mol}^{-1}$$

The reaction in eq 5 is a major fragmentation pathway of the heterocubanes upon electron ionization (after loss of one methyl group).⁷

3.2.1.b. Dissociation of the Trimer 4. The trimer **4** is unstable with respect to the cubane **1** (see above) as well as with respect to the dimer **6**, owing to the increase in entropy:



$$\Delta H^\circ_{298} = 14.9 \text{ kJ mol}^{-1} \quad \Delta G^\circ_{298} = -18.0 \text{ kJ mol}^{-1}$$

On the other hand, the formation of the monomer **10** is unfavorable despite the gain in entropy:

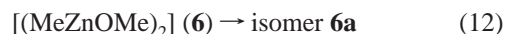


$$\Delta H^\circ_{298} = 228.4 \text{ kJ mol}^{-1} \quad \Delta G^\circ_{298} = 131.9 \text{ kJ mol}^{-1}$$

3.2.1.c. Dissociation of the Dimers. Cleavage of two Zn–O bonds of **6** requires an enthalpy³⁷ of ca. 140 kJ mol⁻¹ whereas the ring opening with formation of the chainlike dimer **6a** is of course less endothermic:



$$\Delta H^\circ_{298} = 142.3 \text{ kJ mol}^{-1} \quad \Delta G^\circ_{298} = 100.0 \text{ kJ mol}^{-1}$$



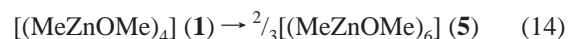
$$\Delta H^\circ_{298} = 92.9 \text{ kJ mol}^{-1} \quad \Delta G^\circ_{298} = 97.8 \text{ kJ mol}^{-1}$$

With bulky alkoxy groups, the dissociation of the dimer into two monomers is considerably more favorable energetically compared to the all-methyl derivative:



$$\Delta H^\circ_{298} = 129.8 \text{ kJ mol}^{-1} \quad \Delta G^\circ_{298} = 76.1 \text{ kJ mol}^{-1}$$

3.2.1.d. Association to the Hexamer. The hexamer **5** is less stable than the cubane **1** but its formation from the trimer is exothermic:



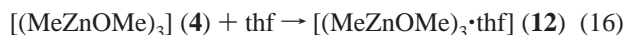
$$\Delta H^\circ_{298} = 33.4 \text{ kJ mol}^{-1} \quad \Delta G^\circ_{298} = 62.6 \text{ kJ mol}^{-1}$$



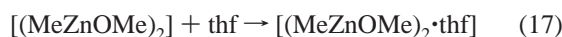
$$\Delta H^\circ_{298} = -51.7 \text{ kJ mol}^{-1} \quad \Delta G^\circ_{298} = +3.2 \text{ kJ mol}^{-1}$$

The Gibbs reaction energy in eq 15 is equivalent to an equilibrium constant $K_c = c^{1/2}(\mathbf{5})/c(\mathbf{4})$ of 0.26 kJ^{-1/2} mol^{1/2} (at 25 °C).

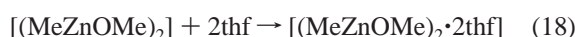
3.2.2. Adduct Formation with Tetrahydrofuran. The NBO atomic charge on the oxygen atom of tetrahydrofuran is -0.61 units, resulting in a dipole moment of 2.02 D. Therefore, this molecule is attracted by the positively charged zinc atoms of the cluster molecules studied in this work. Addition of the first thf molecule liberates an enthalpy of 23–36 kJ mol⁻¹ and the coordination of a second thf produces slightly less energy:



$$\Delta H^\circ_{298} = -29.3 \text{ kJ mol}^{-1} \quad \Delta G^\circ_{298} = +25.8 \text{ kJ mol}^{-1}$$



$$\Delta H^\circ_{298} = -22.8 \text{ kJ mol}^{-1} \quad \Delta G^\circ_{298} = +27.0 \text{ kJ mol}^{-1}$$



$$\Delta H^\circ_{298} = -42.1 \text{ kJ mol}^{-1} \quad \Delta G^\circ_{298} = +51.1 \text{ kJ mol}^{-1}$$

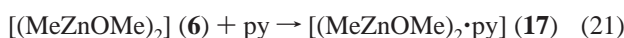


$$\Delta H^\circ_{298} = -35.7 \text{ kJ mol}^{-1} \quad \Delta G^\circ_{298} = +7.8 \text{ kJ mol}^{-1}$$

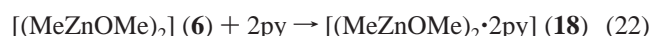


$$\Delta H^\circ_{298} = -55.5 \text{ kJ mol}^{-1} \quad \Delta G^\circ_{298} = +35.3 \text{ kJ mol}^{-1}$$

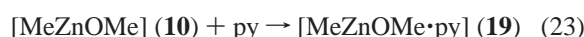
3.2.3. *Adduct Formation with Pyridine.* The calculated dipole moment of pyridine (2.38 D) is larger than that of tetrahydrofuran (2.02 D) although the atomic charge on the nitrogen atom is only -0.46. Nevertheless, the interaction of pyridine with the methylzinc alkoxides is by ca. 65% stronger than in the case of thf, as the following reaction enthalpies demonstrate:



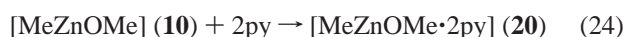
$$\Delta H^\circ_{298} = -35.6 \text{ kJ mol}^{-1} \quad \Delta G^\circ_{298} = +17.5 \text{ kJ mol}^{-1}$$



$$\Delta H^\circ_{298} = -66.9 \text{ kJ mol}^{-1} \quad \Delta G^\circ_{298} = +32.1 \text{ kJ mol}^{-1}$$



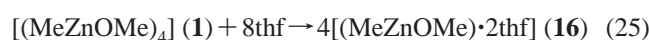
$$\Delta H^\circ_{298} = -51.3 \text{ kJ mol}^{-1} \quad \Delta G^\circ_{298} = -5.8 \text{ kJ mol}^{-1}$$



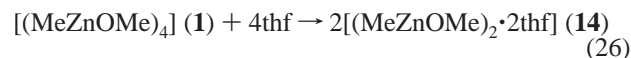
$$\Delta H^\circ_{298} = -81.6 \text{ kJ mol}^{-1} \quad \Delta G^\circ_{298} = -9.5 \text{ kJ mol}^{-1}$$

3.2.4. *Dissociation Reactions of (MeZnOMe)_n Complexes in the Presence of Tetrahydrofuran or Pyridine.* It has been reported that ethylzinc phenoxide is tetrameric in benzene solution but monomeric in dioxane or in benzene if an appropriate amount of pyridine is added.³⁵ These results, obtained by cryoscopic molecular mass determinations, indicate that the adduct formation liberates more (Gibbs) energy than the dissociation of the tetramer into monomers requires. To our knowledge, quantitative data on the thermodynamics of such reactions are missing. Thus, we have calculated the enthalpies and Gibbs energies of the dissociation reactions of the tetramer **1** in the presence of donor solvents, as shown in eqs 25–27. All reactions are endothermic and, more important, strongly endoergonic as a consequence of the decrease in entropy.

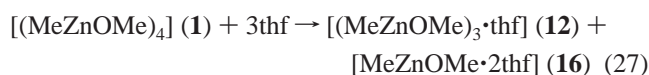
3.2.4.a. *Dissociation with Addition of Tetrahydrofuran.* The following data demonstrate that the interaction with thf molecules is by far not strong enough to overcome the dissociation energy of the cubane, regardless of whether thf adducts of monomers, dimers or trimers are formed:



$$\Delta H^\circ_{298} = 184.7 \text{ kJ mol}^{-1} \quad \Delta G^\circ_{298} = 375.5 \text{ kJ mol}^{-1}$$

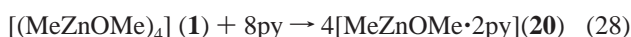


$$\Delta H^\circ_{298} = 38.0 \text{ kJ mol}^{-1} \quad \Delta G^\circ_{298} = 136.4 \text{ kJ mol}^{-1}$$

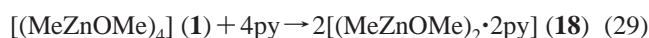


$$\Delta H^\circ_{298} = 93.6 \text{ kJ mol}^{-1} \quad \Delta G^\circ_{298} = 163.3 \text{ kJ mol}^{-1}$$

3.2.4.b. *Dissociation with Addition of Pyridine.* The dissociation of (MeZnOMe)_n complexes on adduct formation with pyridine is exothermic only in the case of the dimer formation, but the negative reaction entropy makes even this reaction endoergonic with the equilibrium completely on the left side of the equation:



$$\Delta H^\circ_{298} = 80.4 \text{ kJ mol}^{-1} \quad \Delta G^\circ_{298} = 272.1 \text{ kJ mol}^{-1}$$



$$\Delta H^\circ_{298} = -11.6 \text{ kJ mol}^{-1} \quad \Delta G^\circ_{298} = +98.4 \text{ kJ mol}^{-1}$$

3.2.5. *Thermolysis Reaction of [(MeZnO^tBu)₂] (7).* Certain zink complexes with bridging isopropoxy or *tert*-butoxy ligands are known to eliminate isopropene and isobutene, respectively, on heating^{6,38} and, among other reactions, also on electron ionization.⁷ Therefore, we have calculated the thermodynamics of the following model reaction:



$$\Delta H^\circ_{298} = 113.4 \text{ kJ mol}^{-1} \quad \Delta G^\circ_{298} = 6.0 \text{ kJ mol}^{-1}$$

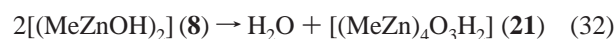
The small value of the Gibbs energy of this reaction in combination with the positive reaction entropy shows that the equilibrium (30) will be on the right side at temperatures slightly above 298 K (exactly at temperatures >367 K).

3.2.6. *Hydrolysis and Condensation Reactions of Me–Zn and Zn–OH Bonds.* Methylzinc compounds are moisture sensitive and produce methane on treatment with water. To determine the thermodynamics of this hydrolysis the following model reaction was studied:



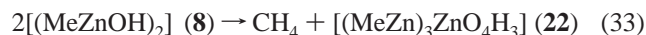
$$\Delta H^\circ_{298} = -73.2 \text{ kJ mol}^{-1} \quad \Delta G^\circ_{298} = -66.1 \text{ kJ mol}^{-1}$$

The four-membered Zn₂O₂ ring of **8** is preserved during this hydrolysis, which eventually will lead to zinc hydroxide. In the absence of water, the hydroxy groups of [(MeZnOH)₂] molecules may react intermolecularly with each other to split off H₂O or with the Me–Zn group of a second molecule with formation of methane. The intermolecular condensation of two OH groups is slightly endothermic and endoergonic:



$$\Delta H^\circ_{298} = 18.7 \text{ kJ mol}^{-1} \quad \Delta G^\circ_{298} = 32.0 \text{ kJ mol}^{-1}$$

In contrast, the methane formation according to eq 33 is strongly exothermic:



$$\Delta H^\circ_{298} = -79.4 \text{ kJ mol}^{-1} \quad \Delta G^\circ_{298} = -65.3 \text{ kJ mol}^{-1}$$

The structures of the two resulting tetranuclear complexes are shown in Figure 9. Compound **21** is spirocyclic and, excepting eight of the twelve methyl-hydrogen atoms, has all atoms in two perpendicular planes (symmetry D_{2d}). A straight line connects the atoms HOOH located on both planes. The bond angles at the four-coordinate oxygen atom are 96.2° within the rings and 116.5° outside the rings. The “double-dimer” **22** consists of two coplanar four-membered rings with all atoms in one plane except the methyl-hydrogen atoms (dipole moment 1.31 D). The most remarkable feature of this species is the very short Zn–O bond of 180.5 pm connecting the two rings.

As a consequence of reaction 33, it can be predicted that the complex $[(\text{MeZnO}^i\text{Bu})_4]$ on heating will first split off isobutene according to eq 30 and the hydroxo complex formed in this reaction may then trigger an intermolecular condensation with formation of methane in analogy to eq 33. In the case of $[(\text{MeZnO}^i\text{Pr})_4]$, propene will be eliminated followed by aggregation to larger complexes.

3.2.7. Disproportionation Reaction. The reaction energy of the remarkable disproportionation reaction shown in eq 1 was calculated at the B3LYP/6-31+G*/B3LYP/6-31G* level because the molecular size of the dicubane $\text{Zn}(\text{L1})_2$ with its 400 electrons prevented a higher level of theory. The reaction enthalpy of this equilibrium is small and positive ($\Delta E = +38.9 \text{ kJ mol}^{-1}$). The calculated Gibbs reaction energy of 50.8 kJ mol^{-1} results in a very small equilibrium constant of ca. 10^{-8} (at 60°C). The experimental equilibrium constant for the reaction in eq 1, $K_c = c[\text{Me}_2\text{Zn}] \cdot c[\text{Zn}\{(\text{MeZn})_3(\text{OMe})_4\}_2] / c^2[(\text{MeZnOMe})_4]$, has been reported as 0.076(16) at 60°C and was shown to be independent of temperature ($40\text{--}80^\circ\text{C}$) and concentration (5–12% by mass).²⁷ At 25°C , the equilibrium is established within 40 h. From the lacking temperature dependence it was estimated that the enthalpy of the reaction in eq 1 must be smaller than $+4 \text{ kJ mol}^{-1}$.²⁷ The experimental equilibrium constant is equivalent to a Gibbs reaction energy ΔG°_{333} of $+6.9 \text{ kJ mol}^{-1}$. Thus, the agreement between the calculated and experimental data is only fair in this case, which may be rationalized by the large size of the involved molecules making accurate energy calculations difficult.

The binding energy between the zinc dication and the two chelating ligands of **3** is extremely high but still much smaller than the lattice energy of zinc oxide (4033 kJ mol^{-1}).³⁹ At the B3LYP/6-31+G*/B3LYP/6-31G* level we obtained the following reaction energy:



3.3. Possible Mechanisms for the Ligand Exchange, Interconversion and Disproportionation Reactions of $[(\text{MeZnOMe})_n]$ Clusters. If two tetrameric clusters $[(\text{RZnOR}')_4]$ ($\text{R}, \text{R}' = \text{Me}, \text{Et}$) containing different alkoxy groups are mixed in solution, a slow exchange of the ligands R' (or OR') is observed.^{24,40} In the following we discuss several possible routes for this ligand exchange, which has been monitored by ^1H NMR and mass spectroscopy. In this context it is also of interest to find out how hexamers can be formed from tetramers and how the disproportionation reaction in eq 1 takes place in which two sterically well protected tetramers seem to attack each other.

3.3.1. Dissociation Reactions. If two different tetramers $[(\text{RZnOR}')_4]$ are mixed in solution and both are assumed to dissociate to smaller units that then recombine to form mixed

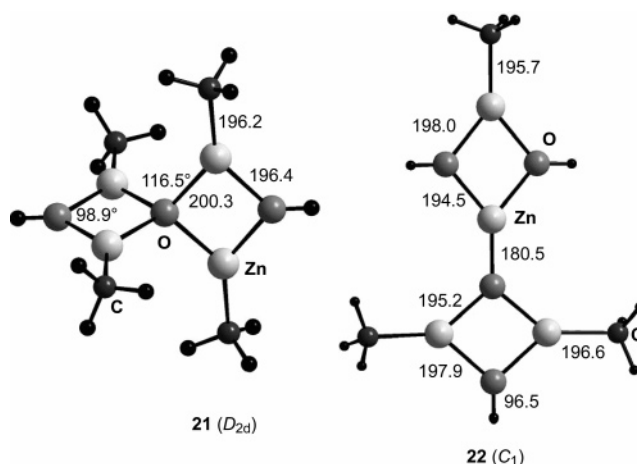


Figure 9. Structures of the tetranuclear condensation products $[(\text{MeZn})_4\text{O}_3\text{H}_2]$ (**21**) and $[(\text{MeZn})_3\text{ZnO}_4\text{H}_3]$ (**22**). Bond lengths in pm.

tetramers, a ligand exchange results. Above we have shown that of all dissociation reactions the cleavage into dimers is most favorable energetically. The Gibbs energy of reaction 6 is 34.2 kJ mol^{-1} , which is equivalent to an equilibrium constant K_c of $5.9 \times 10^{-7} \text{ mol L}^{-1}$ for the tetramer (**1**)–dimer (**6**) equilibrium at 25°C . At a cubane concentration of 0.10 mol L^{-1} the dimer concentration at equilibrium will be $2.4 \times 10^{-4} \text{ mol L}^{-1}$. At lower cubane concentrations or higher temperatures the equilibrium (**6**) will shift more and more to the side of the dimer. Our calculated dimer concentration is probably sufficient to explain the observed ligand exchange reaction provided the activation energy of the dissociation reaction is not too large. Because the reaction enthalpy for the formation of dimers from tetramers **1** is 122 kJ mol^{-1} , the activation enthalpy may be of the same order of magnitude (or higher). The ladder-shaped tetramer **1a** is expected to be an intermediate in the dissociation reaction of cubanes to dimers. In the case of the *tert*-butyl-substituted cubane **2** the activation energy may be lower than 100 kJ mol^{-1} because the enthalpy of dissociation is considerably lower than for **1**; see eq 7.

If very strong Lewis bases are present in solution, the tetramer–dimer equilibrium is expected to shift toward the dimer because the tetramer does not interact with Lewis bases equally strongly. In this case, catalytic ligand exchange reaction via dimers is possible. Our data show, however, that neither tetrahydrofuran nor pyridine is a strong enough Lewis base to cleave tetramer **1** into dimers at room temperature. This result is in agreement with the observations by Coates and Ridley who failed to prepare any adduct by cooling a mixture of **1** and pyridine.³⁴ However, the preparation of the dimeric complexes $[(\text{EtZnOPh})_2 \cdot 2\text{py}]$ and $[(\text{EtZnOC}_6\text{F}_5)_2 \cdot 2\text{py}]$ ¹² mentioned above has shown that pyridine is strong enough to stabilize these particular dimers over the cubanes. Evidently, the dissociation energy of the phenoxy-substituted cubanes to the corresponding dimers is considerably lower than for the methoxy derivatives. This view is supported by our finding that the dissociation of **2** into dimers is by 33 kJ mol^{-1} more favorable than the corresponding dissociation of **1**. In addition, the phenoxy derivatives may be stronger acceptors than the methoxy-substituted dimers. It is interesting to note that $[(\text{MeZnOMe})_2 \cdot 2\text{py}]$ has not been prepared yet.

In this context the large dipole moments of some of the tetrahydrofuran and pyridine adducts should be mentioned. Such highly polar species will be stabilized in solvents of high

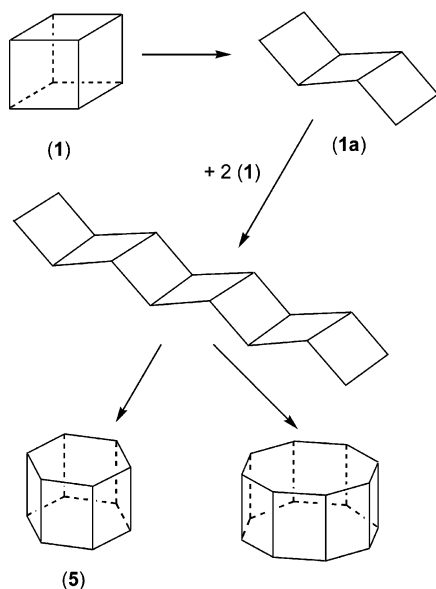


Figure 10. Possible routes for the formation of hexamers and octamers from the cubane **1** via the ladder-type isomer **1a**. Methyl groups have been omitted for clarity. The proposed reactions are assumed to be reversible.

dielectric constant (such as pure thf and py), shifting the corresponding equilibrium reactions more to the side of the adducts.

3.3.2. Association Reactions. Some complexes of the type $[(\text{RZnOR}')_n]$ exist as hexamers or even octamers in solution.¹² Above it was shown that the enthalpy difference between $[(\text{MeZnOMe})_4]$ and $2/3[(\text{MeZnOMe})_6]$ is only 33.4 kJ mol⁻¹ or 8.4 kJ per mol of zinc atoms. How can these larger clusters be formed from the tetramer? The most likely route involves the opening of the cubane to form the ladder-type isomer **1a** (Figure 1), which then may grow by incorporation of a second and a third cubane molecule (or by addition of dimers). From this extended ladder structure the drum-shaped hexamers and octamers can be split off in reactions similar to the reversal of the opening of the cubane; see Figure 10.

If two cubanes having differing alkoxy groups, e.g., $[(\text{MeZnOR})_4]$ and $[(\text{MeZnOR}')_4]$, are mixed, an extended ladder of composition $[(\text{MeZnOR/R}')_n]$ may be formed, possessing a mixture of the two alkoxy groups. Because this process must be reversible, it can be shown that the back-reaction can produce cubanes with differing alkoxy groups in one molecule. In other words, ligand exchange can take place by this mechanism. The corresponding activation energy will probably not be much larger than the enthalpy needed to form the ladder-type isomer from the cubane, i.e., ca. 70 kJ mol⁻¹. In other words, this mechanism may be more favorable thermodynamically and kinetically than the dissociation of tetramers to dimers to explain the ligand exchange reaction. From the ladder-type intermediate hexamers with two different alkoxy groups can be split off, too.

3.3.3. Disproportionation Reaction. One of the most interesting reactions in the chemistry of zinc is the disproportionation reaction shown in eq 1, resulting in the dicubane $[\text{Zn}_7\text{Me}_6(\text{OMe})_8]$ (**3**) with a nearly octahedrally coordinated central atom. If two different cubane molecules $[(\text{MeZnOR})_4]$ and $[(\text{MeZnOR}')_4]$ are mixed, the result may be a dicubane with differing alkoxy groups. Here we discuss whether this mixed dicubane could be an intermediate in the ligand exchange reaction between two different cubane complexes. It is known that octahedral chelate complexes undergo intramolecular ligand scrambling reactions, which result in a racemization at room

temperature if the original complex has been chiral. Several mechanisms have been proposed for this process.⁴¹ If such a scrambling process would operate in the case of a mixed dicubane also, an exchange of the differing alkoxy ligands would take place and the back-reaction of eq 1 would then produce two cubanes with differing alkoxy groups in each molecule. There is, in fact, NMR spectroscopic evidence for a scrambling motion of the -OMe groups in the dicubane **3**: the chemical shift of the methyl protons of the methoxy groups adjacent to the hexacoordinate Zn atom is temperature dependent whereas those of the other methyl and methoxy groups are not.²⁷

On the other hand, we have shown above that dicubane molecules with sterically demanding alkoxy groups would not be stable due to repulsion between these groups at the octahedral center. Thus, the equilibrium shown in eq 1 is expected to be completely on the left side if *all* -OMe groups in one of the cubane molecules are replaced by -OⁱPr or -OⁱBu, for instance. This view is supported by the following experimental observation. If the heterocubane **1** and Me_2Zn are mixed at room temperature in toluene, a slow exchange of the methyl groups of both molecules takes place, as indicated by the occurrence of just *one* broad methyl signal in the ¹H NMR spectrum. This exchange process can be sped up by heating to 60 °C (1 sharp methyl signal) and can be frozen by cooling to 0 °C (2 methyl signals).²⁴ Most likely, the methyl exchange at the zinc atoms takes place via the reversible formation and decomposition of the dicubane **3** according to eq 1. The interesting finding is now that no such exchange takes place if Me_2Zn is mixed with either $[(\text{MeZnO}^i\text{Pr})_4]$ or $[(\text{MeZnO}^i\text{Bu})_4]$.²⁴ Evidently, the corresponding dicubanes with eight sterically demanding alkoxy groups are unstable. However, if only one or two such groups are present in the particular dicubane, there should be no steric problems and the exchange of alkoxy groups between two heterocubane molecules as described above may be explained on this basis.

What could be the mechanism for the disproportionation reaction in eq 1? The cubane molecules **1** are sterically rather protected and have to be opened or dissociated first to be able to react with each other with formation of Me_2Zn and **3**. To cleave one Zn-O bond of **1** requires probably ca. 36 kJ mol⁻¹, half the energy needed to cleave two parallel Zn-O bonds of **1** with formation of isomer **1a**. To cleave the four parallel Zn-O bonds of **1** requires ca. 122 kJ mol⁻¹, as can be concluded from the data in eq 6. Thus, there are several possibilities. The most energy efficient reaction is probably the opening of one Zn-O bond of a cubane molecule followed by methylation of the resulting three-coordinate zinc atom by a second cubane molecule with elimination of Me_2Zn and "condensation" of the two cubane units to form the dicubane.

It is interesting to note that similar disproportionation reactions with elimination of Me_2Zn may also occur on heating of other methylzinc alkoxide complexes. For the further elucidation of the ligand exchange and disproportionation reactions, the activation energy and reaction order of these reactions should be determined experimentally.

4. Summary and Conclusions

For the first time it has been shown that tetrameric, trimeric and dimeric complexes $[(\text{MeZnOMe})_n]$ exist as several isomers on the particular potential energy surfaces. The global minimum structures are the cubanelike tetramer, a roof-shaped trimer and a cyclic dimer, but a ladder-type tetramer and a chainlike dimer are of relative energies that are less than 90 kJ mol⁻¹ higher than the energies of the global minimum structures. Monomeric

[MeZnOMe] is slightly bent at the zinc atom. The hexameric complex [(MeZnOMe)₆] is drum-shaped and only slightly less stable than the cubane tetramer; thus, it may be formed on heating the tetramer. The Zn–O bonds within these multinuclear clusters are longer (weaker and softer) than the Zn–O bond in the monomer [MeZnOMe]. For the same reason, exocyclic Zn–O bonds are shorter than Zn–O bonds within the clusters. Dissociation of the heterocubanes [(MeZnOMe)₄] and [(MeZnO^t-Bu)₄] to trimers, dimers or monomers is strongly endothermic, but least of all in the case of dimer formation. Bulky substituents lower the dissociation enthalpies.

The NBO atomic charges on the zinc atoms of [(MeZnOMe)_n] complexes decrease with decreasing cluster size from +1.48 electrostatic units in the hexamer, via +1.46 in the tetramer and +1.45 in the dimer to +1.36 in the monomer. In the same order the charges on the oxygen atoms decrease from −1.14 (hexamer) via −1.12 (tetramer and dimer) to −1.04 (monomer). In other words, the polarity of the Zn–O bonds increases with the cluster size. The Zn–C bonds are also highly polar.

Coordination of tetrahydrofuran (thf) to trimeric, dimeric or monomeric complexes is exothermic, but the energy released is not sufficient to break up the multinuclear clusters to form thf adducts of smaller units. However, the thf coordination weakens the Zn–O bonds within the clusters. The interaction is explained by ion–dipole attraction. The binding energy of pyridine to [(MeZnOMe)_n] complexes is about 65% larger than that of thf. However, this interaction is still not strong enough to break up the methylated heterocubane to form a dimer·2py adduct, for instance.

The hydrolysis of Zn–Me bonds with formation of methane is strongly exothermic. In contrast, the intermolecular condensation of the resulting Zn–OH groups with formation of water is slightly endothermic. The thermal elimination of isobutene from Zn–O^tBu groups with formation of Zn–OH groups is endothermic, but the corresponding Gibbs reaction energy at 25 °C is very small. This reaction is predicted to be followed by an intermolecular condensation between Zn–OH and Me–Zn groups with elimination of methane.

The disproportionation of [(MeZnOMe)₄] to dimethylzinc and the dicubane [Zn{(MeZn)₃(OMe)₄}]₂ is less endothermic than any other potential thermal reaction of the heterocubane **1**, i.e., less than any isomerization or dissociation reaction. However, dicubane molecules with –OⁱPr or –O^tBu substituents rather than –OMe are predicted to be unstable. For thermodynamic reasons, ligand exchange, interconversion and disproportionation reactions of Zn₄O₄ heterocubane clusters may be explained mechanistically via isomer formation rather than by reversible dissociation to dimers.

Acknowledgment. We appreciate stimulating discussion with Matthias Driess who suggested this work, as well as the assistance of Bernd Kallies at Norddeutscher Verbund für Hoch- und Höchstleistungsrechnen (HLRN). This work has been supported by HLRN, by the Deutsche Forschungsgemeinschaft and by Grillo AG.

Supporting Information Available: Electronic energies, enthalpies and Gibbs energies, fundamental vibrations of (MeZnOMe)₂, as well as Cartesian coordinates of all calculated zinc complexes. This material is available free of charge via the Internet at <http://pubs.acs.org>.

References and Notes

- (1) Auld, J.; Houlton, D. J.; Jones, A. C.; Rushworth, S. A.; Malik, M. A.; O'Brien, P.; Critchlow, G. W. *J. Mater. Chem.* **1994**, *4*, 1249.
- (2) Hambrock, J.; Rabe, S.; Merz, K.; Birkner, A.; Wohlfart, A.; Fischer, R. A.; Driess, M. *J. Mater. Chem.* **2003**, *13*, 1731. Polarz, S.; Neues, F.; van den Berg, M. W. E.; Grünert, W.; Khodeir, L. *J. Am. Chem. Soc.* **2005**, *127*, 12028. Polarz, S.; Roy, A.; Merz, M.; Halm, S.; Schröder, D.; Schneider, L.; Bacher, G.; Kruis, F. E.; Driess, M. *Small* **2005**, *1*, 540.
- (3) Olmstead, M. M.; Power, P. P.; Shoner, S. C. *J. Am. Chem. Soc.* **1991**, *113*, 3379.
- (4) van der Schaaf, P. A.; Wissing, E.; Boersma, J.; Smeets, W. J. J.; Spek, A. L.; van Koten, G. *Organometallics* **1993**, *12*, 3624.
- (5) Erxleben, A. *Inorg. Chem.* **2001**, *40*, 208.
- (6) Schön, E.; Plattner, D. A.; Chen, P. *Inorg. Chem.* **2004**, *43*, 3164.
- (7) Schröder, D.; Schwarz, H.; Polarz, S.; Driess, M. *Phys. Chem. Chem. Phys.* **2005**, *7*, 1049.
- (8) Driess, M.; Merz, K.; Rell, S. *Eur. J. Inorg. Chem.* **2000**, 2517.
- (9) Merz, K.; Hu, H.-M.; Rell, S.; Driess, M. *Eur. J. Inorg. Chem.* **2003**, 51.
- (10) Coates, G. E.; Ridley, D. *J. Chem. Soc.* **1965**, 1870.
- (11) Shearer, H. M. M.; Spencer, C. B. *Acta Crystallogr.* **1980**, *B36*, 2046.
- (12) Noltes, J. G.; Boersma, J. *J. Organomet. Chem.* **1968**, *12*, 425.
- (13) Frisch, M. J.; Trucks, G. W.; Schlegel, H. B.; Scuseria, G. E.; Robb, M. A.; Cheeseman, J. R.; Montgomery, J. A., Jr.; Vreven, T.; Kudin, K. N.; Burant, J. C.; Millam, J. M.; Iyengar, S. S.; Tomasi, J.; Barone, V.; Mennucci, B.; Cossi, M.; Scalmani, G.; Rega, N.; Petersson, G. A.; Nakatsuji, H.; Hada, M.; Ehara, M.; Toyota, K.; Fukuda, R.; Hasegawa, J.; Ishida, M.; Nakajima, T.; Honda, Y.; Kitao, O.; Nakai, H.; Klene, M.; Li, X.; Knox, J. E.; Hratchian, H. P.; Cross, J. B.; Bakken, V.; Adamo, C.; Jaramillo, J.; Gomperts, R.; Stratmann, R. E.; Yazyev, O.; Austin, A. J.; Cammi, R.; Pomelli, C.; Ochterski, J. W.; Ayala, P. Y.; Morokuma, K.; Voth, G. A.; Salvador, P.; Dannenberg, J. J.; Zakrzewski, V. G.; Dapprich, S.; Daniels, A. D.; Strain, M. C.; Farkas, O.; Malick, D. K.; Rabuck, A. D.; Raghavachari, K.; Foresman, J. B.; Ortiz, J. V.; Cui, Q.; Baboul, A. G.; Clifford, S.; Cioslowski, J.; Stefanov, B. B.; Liu, G.; Liashenko, A.; Piskorz, P.; Komaromi, I.; Martin, R. L.; Fox, D. J.; Keith, T.; Al-Laham, M. A.; Peng, C. Y.; Nanayakkara, A.; Challacombe, M.; Gill, P. M. W.; Johnson, B.; Chen, W.; Wong, M. W.; Gonzalez, C.; Pople, J. A. *Gaussian 03*, revision C.02; Gaussian, Inc.: Wallingford CT, 2004.
- (14) Curtiss, L. A.; Redfern, P. C.; Raghavachari, K.; Pople, J. A. *J. Chem. Phys.* **2001**, *114*, 108.
- (15) Reed, A. E.; Curtiss, L. A.; Weinhold, F. *Chem. Rev.* **1988**, *88*, 899.
- (16) Messerschmidt, M.; Wagner, A.; Wong, M. W.; Luger, P. *J. Am. Chem. Soc.* **2002**, *124*, 732.
- (17) Almendinger, A.; Helgaker, T. U.; Haaland, A.; Samdal, S. *Acta Chem. Scand.* **1982**, *A36*, 159.
- (18) (a) Jackson, R. L. *Chem. Phys. Lett.* **1989**, *163*, 315. (b) McMillen, D. F.; Golden, D. M. *Amu. Rev. Phys. Chem.* **1982**, *33*, 493. (c) Smith, G. P.; Patrick, R. *Int. J. Chem. Kinet.* **1983**, *15*, 167.
- (19) The symmetry of the global minimum structure of Me₂Zn depends somewhat on the basis set. Although *D*_{3h} symmetry is obtained with the bases 6-31G* and 6-31G(2df,p), the lower *D*₃ symmetry with a torsion angle between the methyl groups of 23.3° is obtained at the 6-31+G* level. In each case, the molecule is linear with all vibrational frequencies real. The energy difference between the *D*_{3h} and *D*₃ structures at the 6-31+G* level is negligible (*D*_{3h} is a first-order transition state). In other words, there is practically free rotation about the Zn–C bonds, in agreement with experiment. At the 3-21G* level the molecule is bent (C–Zn–C = 159.4°; *C*_{2v} symmetry).
- (20) Coats, A. M.; McKean, D. C.; Starcke, C.; Thiel, W. *Spectrochim. Acta A* **1995**, *51*, 685. Coats, A. M.; McKean, D. C.; Edwards, H. G. M.; Fawcett, V. J. *Mol. Struct.* **1994**, *320*, 159. Bochmann, M.; Chesters, M. A.; Coleman, A. P.; Grinter, R.; Linder, D. R. *Spectrochim. Acta A* **1992**, *48*, 1173.
- (21) Rao, K. S.; Stoicheff, B. B.; Turner, R. *Can. J. Phys.* **1960**, *38*, 1516.
- (22) Antes, I.; Frenking, G. *Organometallics* **1995**, *14*, 4263.
- (23) Matxain, J. M.; Fowler, J. E.; Ugalde, J. M. *Phys. Rev. A* **2000**, *62*, 053201.
- (24) Jeffery, E. A.; Mole, T. *Aust. J. Chem.* **1968**, *21*, 1187.
- (25) Geerts, R. L.; Huffman, J. C.; Caulton, K. G. *Inorg. Chem.* **1986**, *25*, 1803.
- (26) Allen, G.; Bruce, J. M.; Farren, D. W.; Hutchinson, F. G. *J. Chem. Soc. B* **1966**, 799.
- (27) Eisenhuth, W. H.; Van Wazer, J. R. *J. Am. Chem. Soc.* **1968**, *90*, 5397.
- (28) Ziegler, M. L.; Weiss, J. *Angew. Chem.* **1970**, *82*, 931; *Angew. Chem., Int. Ed. Engl.* **1970**, *9*, 905.
- (29) Gorrell, I. B.; Looney, A.; Parkin, G.; Rheingold, A. L. *J. Am. Chem. Soc.* **1990**, *112*, 4068.
- (30) Adler, B.; Lachowitz, A.; Thiele, K. H. *Z. Anorg. Allg. Chem.* **1976**, *423*, 27.

- (31) Wang, X.; Andrews, L. *J. Phys. Chem. A* **2005**, *109*, 3849.
- (32) The tilt is defined as the deviation of the approximate C_3 axis of the methyl group from the direction of the C–X bond (in the present case: C–Zn and C–O bonds).
- (33) Pross, A.; Radom, L.; Riggs, N. V. *J. Am. Chem. Soc.* **1980**, *102*, 2253.
- (34) Coates, G. E.; Ridley, D. *J. Chem. Soc. A* **1966**, 1064.
- (35) Górecki, P.; Kuran, W. *J. Organomet. Chem.* **1984**, *265*, 1 and references therein.
- (36) van der Schaaf, P. A.; Wissing, E.; Boersma, J.; Smeets, W. J. J.; Spek, A. L.; van Koten, G. *Organometallics* **1993**, *12*, 3624.
- (37) By the BP86/6-311++G* method, the dissociation enthalpy (ΔH°_{298}) for the reaction $\mathbf{6} \rightarrow 2 \times \mathbf{10}$ is predicted as 135.6 kJ mol⁻¹.
- (38) Ashby, E. C.; Willard, G. F.; Goel, A. B. *J. Org. Chem.* **1979**, *44*, 1221.
- (39) Waddington, T. C. *Adv. Inorg. Chem. Radiochem.* **1959**, *1*, 157.
- (40) Polarz, S. Personal communication 2005.
- (41) Kepert, D. L. *Inorg. Chem.* **1977**, *23*, 1.